Structure and Properties of U(IV) and Np(IV) Selenium Bis(phenolate) Complexes and Their Reaction with p-Benzoquinone

SCHOLARONE™
Manuscripts

ROYAL SOCIETY OF CHEMISTRY

Chemical Communications

COMMUNICATION

Structure and Properties of [(4,6-tBu2C6H2O)2Se]2An(THF)2, An = U, Np, and Their Reaction with *p*-Benzoquinone

Alexander J. Myers,[ab] Pokpong Rungthanaphatsophon,[a] Andrew C. Behrle,[a] Sean P. Vilanova,[a] Stephen P. Kelley,[a] Wayne W. Lukens,*[b] and Justin R. Walensky*[a]

The synthesis and characterization of U(IV) and Np(IV) selenium bis(phenolate) complexes are reported. The reaction of two equivalents of the U(IV) complex with *p*-benzoquinone results in the formation of a U(V)-U(V) species with a bridging reduced quinone. This represents rare examples of high-valent uranium chemistry as well as a rare example of a neptunium aryloxide complex.

The coordination chemistry and reactivity of the actinides offer insight into their structure and bonding, which in turn improves our understanding of the behaviour of these elements especially with regard to the nuclear fuel cycle. Transuranic actinides are particularly understudied even compared with lighter actinides due to the difficulty in obtaining these elements and the infrastructure required to handle these elements safely.

Alkoxide and aryloxide ligands have served a significant role in advancing our understanding of actinide chemistry. The highly electronegative oxygen atoms provide a more ionic interaction with the actinide which enhances the stability of the resulting complexes. Oxygen-based ligands have demonstrated the ability to isolate complexes with U(II),[1] U(III),[2-4] U(V),[5] and U(VI),[6] but especially with respect to tetravalent actinides.[7-12]

We recently examined the structure of diamagnetic complexes with the selenium bis(phenolate) ligand, $[(4,6-^tBu_2C_6H_2O)_2Se]^{2-}$, $^{Ar}OSeO^{Ar}$.[13] This dianionic, chelating ligand effectively stabilizes tetravalent metal complexes of Ti, Zr, Hf, Ce, and Th, and we endeavoured to extend this study to uranium and neptunium. Herein, we report the synthesis of the U(IV) and Np(IV) complexes. The reactivity of these complexes with *p*-benzoquinone has been explored. With U(IV), this reaction affords a dinuclear U(V)-U(V) compound bridged by *p*-hydroquinone dianion. However, the addition of *p*-benzoquinone to the Np(IV) species produces no reaction. The magnetic, spectroscopic, and structural properties of these complexes are detailed.

The salt metathesis reaction of UCl_4 with two equivalents of $K_2(^{Ar}OSeO^{Ar})$ in THF resulted in an emerald green solution, eqn (1). The ^{1}H NMR spectrum showed paramagnetically shifted resonances between 15.2 and -10.3 ppm. X-ray quality crystals were grown

a. Department of Chemistry, University of Missouri, Columbia, USA
  Email: WalenskyJ@missouri.edu
b. Chemical Sciences Division, Lawrence Berkeley National Laboratory, Berkeley, California 94720, USA.
  Email: wwlukens@lbl.gov
† Electronic Supplementary Information (ESI) available: [details of any supplementary information available should be included here]. See DOI: 10.1039/x0xx00000x

from a saturated toluene solution at -20 °C. Analysis of a single crystal revealed the U(IV) complex, $U[^{Ar}OSeO^{Ar}]_2(THF)_2$, **1**, Figure S11. The THF molecules in complex **1** are labile, and when exposed to vacuum for extended periods of time, the unsolvated complex is observed by ^{1}H NMR spectroscopy.

$$2 K_2^{Ar}OSeO^{Ar} + AnCl_4(DME)x \xrightarrow[- 4 KCl]{THF} \quad (1)$$

An = U, x = 0; 1
Np, x = 2; 2
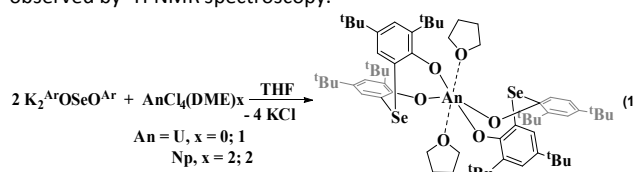
Similar to the previously reported thorium analogue, **1** displays a highly distorted octahedral geometry where the phenolic oxygen atoms are cis to one another.[13] Additionally, one selenium atom is above the aromatic rings while the other is below. The U-O$_{phenoxide}$ bond distances range from 2.185(4)-2.223(4) Å and compare well with other uranium aryloxide complexes. For example, $U(O-2,6-^tBu-C_6H_3)_4$[14] and $[U(salan-^tBu_2)_2]$[10] have U-O bond distances of 2.135(4) Å and 2.219(2)-2.263(2) Å, respectively. The U-Se distances are 3.2606(6) and 3.1642(6) Å, which are longer than the sum of the covalent radii (Σ = 2.86 Å)[15] suggesting no interaction exists between the selenium atom and the uranium centre.

The magnetic susceptibility of **1** is typical of U(IV). The magnetic moment of the ground state can be determined from the value of χT vs T extrapolated to 0 K. For **1**, χT is zero at 0 K, so the ground state is a singlet and only displays temperature independent magnetism, which is typical for U(IV) in low symmetry. χT is linear in T to 20 K, which indicates that the first excited state is approximately 40 to 60 K (27 to 40 cm^{-1}) above the ground state.

The nominal ground state of U(IV) is $^3H_4$ in Russell-Saunders coupling. Bonding in U(IV) is expected to be largely ionic due to poor energy match between the metal and ligand orbitals. The Russell-Saunders ground state of U(IV), $^3H_4$, is split by the ligand field into 9 substates characterized by m_J = 4, 3, 2...-4, which will be mixed by the crystal field due to the ligands. The free ion moment of $^3H_4$ when all the m_J substates are equally thermally populated, is 3.6 μ_B, which is considerably greater than that of **1** at room temperature, 2.5 μ_B. The low value of μ_{eff} for **1** indicates that the total splitting of $^3H_4$ ground state by the crystal field is greater than kT at room temperature (200 cm^{-1}).

The synthesis of $Np[^{Ar}OSeO^{Ar}]_2(THF)_2$, **2**, as a yellow powder, was achieved using a similar route as for **1**, eqn (1). Crystallization from a concentrated toluene solution at -35 °C gave X-ray quality crystals, Figure 1. The structural characterization of **2** revealed a six-coordinate, highly distorted octahedral Np^{4+} metal centre nearly isomorphous with **1**. Like **1**, the selenium bis(phenolate) ligands are

arranged with the phenolic oxygen atoms *cis* to one another. The $Np-O_{phenoxide}$ bonds range from 2.168(9) to 2.228(11) Å and are shorter than the Np-O bonds found in the β-diketonate $Np(FOD)_4$, (FOD = 6,6,7,7,8,8,8-heptafluoro-2,2-dimethyl-3,5-octanedione), 2.290(7)-2.347(5) Å[16] and slightly longer than the Np-O bond distance in $(C_5H_5)_3Np(OPh)$, 2.136(7) Å.[17] The $Np-O_{phenoxide}$ bond lengths in **2** are also much shorter compared to Np(IV) glutaroimide-dioxime complexes recently reported at 2.355(2) and 2.350(2) Å and between 2.389(2)-2.405(2) Å.[18] The Np-Se distances of 3.1289(15) and 3.2287(17) Å are larger than the sum of the covalent radii of 2.87 Å[15] as observed for **1**. Despite the prevalence of actinide aryloxide complexes,[7] the only other structurally characterized neptunium alkoxide or aryloxide is $(C_5H_5)_3Np(OPh)$.
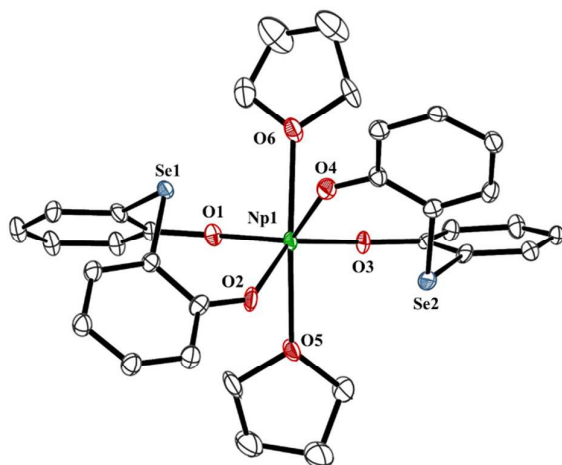

Figure 1. Thermal ellipsoid plot of one of the two independent molecules of **2** shown at the 50% probability level; the other molecular is very similar. The O2-Np-O4 angles are 81.8(4)° in each molecule. The *tert*-butyl groups, hydrogen atoms, and solvent toluene molecules have been omitted for clarity.

The magnetization of **2** decreases sharply at low temperatures, as illustrated in Figure 2. However, the field dependent at low temperature indicates that the decrease is due to saturation rather than coupling. The data of **2** from 25 K to 150K at magnetic fields 0.1 T, 0.5 T, 1 T and 2 T were used to determine the magnetic susceptibility of 1.67 μ_B at 0 K. The Russell-Saunders coupling ground state of Np(IV), $^4I_{9/2}$, is split by the ligand field into 10 substates characterized by m_J = 9/2, 7/2, 5/2...-9/2, which will be mixed by the crystal field due to the ligands. Once the ligand field is considered, the $^4I_{9/2}$ state will split into 5 Kramers doublets. In **2**, the first energy of the first excited doublet is approximately 200 - 300 cm^{-1} above the ground state as determined from the temperature at which the plot of χT *vs. T* deviates from linearity. Interestingly, the first excited state in the Np(IV) compound is much higher in energy than the first excited state in U(IV). Although Np(IV) complexes have the potential to exhibit single molecule magnet behaviour,[19,20] **2** does not display a hysteresis in the magnetization *vs.* field measurements at 2K, Figure S5.

The EPR spectrum of **2** is shown in Figure 3 along with spectrum simulated using EasySpin[21] and the parameters given in Table S4. The sharp feature at 300 mT (g = 2) is due to a minor contribution from organic radical impurities. The simulated spectrum is in general agreement with the experimental spectrum. The largest discrepancy is the position of the two peaks at ~175 mT and ~190

mT. In addition, the linewidths of the features above 400 mT are too narrow in the simulation. Given these differences, it is possible that the simulation represents a local minimum rather than the best fit; however, the largest g and A values, 2.85 and 5134 MHz must be close to the correct values due to the position of the low field peaks. The g-values are related to μ_{eff} of the ground state by $4\mu_{eff}^2 = g_1^2 + g_2^2 + g_3^3$ for effective spin = 1/2. In **2**, the EPR spectrum is consistent with a ground state magnetic moment of 1.65 μ_B, which is in excellent agreement with the value determined by magnetic susceptibility, 1.67 μ_B.
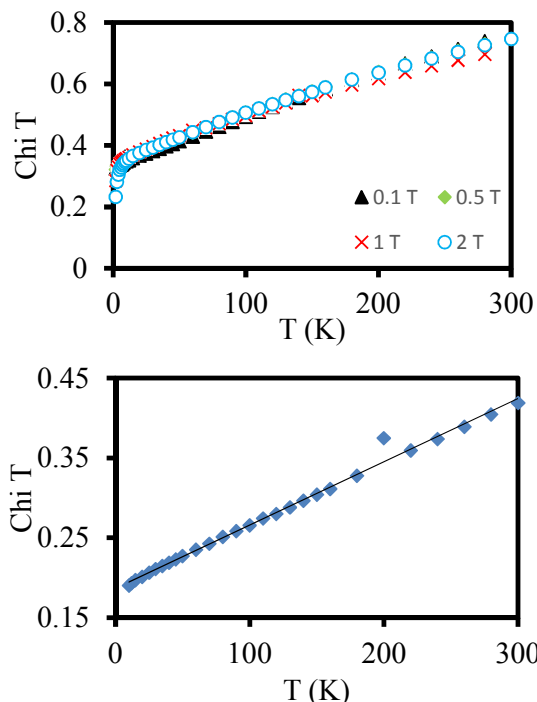
Figure 2. Variable temperature magnetic susceptibility of **2** from 10 K to 300 K (top) and **3** at 1T from 10 K to 300 K (bottom).
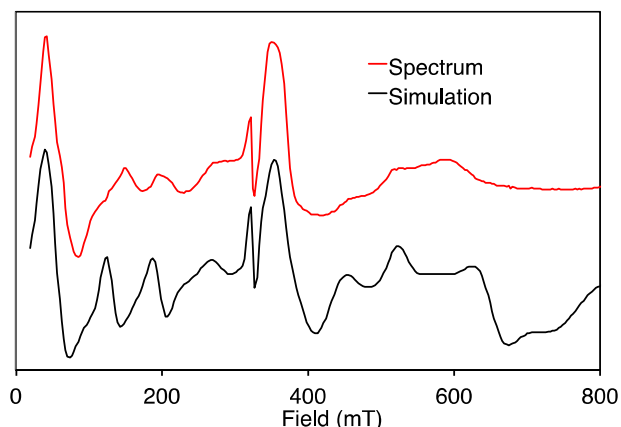

Figure 3. EPR spectrum and simulation for **2**. The 300 mT (g = 2) signal has 0.04% of the intensity of the Np-237 signal.

While Np(IV) is generally EPR active, EPR studies of Np(IV) compounds are rare.[22-31] The paucity of EPR studies is due in part to the very strong hyperfine coupling between the unpaired electron and the large nuclear moment of Np. Accurate determination of the

spin Hamiltonian parameters g and A from the fields of spin transitions requires use of the Breit-Rabi formula.[25] For simulation of the spectrum, diagonalization of the full spin Hamiltonian is required, which was accomplished here using EasySpin.[21] As noted by Poirot et al.,[23] the values of A_i/g_i are relatively constant for Np(IV) and vary from 1807 MHz to 1869 MHz. In **2**, these values are 1779 MHz, 1995 MHz, and 1805 MHz. The first and last are in the range expected for Np(IV) although the value of 1995 MHz is slightly greater than expected. The discrepancy likely indicates the uncertainty in the g and A values for this component, 1.632 and 3256.5 MHz, respectively. Attempting to change either g or A for this component resulted in a much poorer simulation of the experimental spectrum. While the g-values can reveal details of the electronic structures of Np complexes,[23,25,26,28,31-33] this typically requires at least axial symmetry for meaningful discussion. The low symmetry of the Np(IV) site in **2** precludes such an analysis.

Inspired by the use of p-benzoquinone to oxidize Ce(III) to Ce(IV),[34,35] as well as uranium bridging quinone structures,[36] the reaction of **1** with 0.5 equivalents of p-benzoquinone was examined. It resulted in a colour change from green to black. The ^{1}H NMR spectrum showed four resonances ranging from 9.73-1.25 ppm. Black, X-ray quality crystals were grown from a concentrated solution of toluene to reveal the structure as {U[^{Ar}OSeO^{Ar}]$_2$(THF)}$_2$(μ_2-OC$_6$H$_4$O), **3**, Figure 4. The structure of **3** has the same coordination as **1** except for the addition of the bridging benzoquinone and loss of one THF molecule. To confirm the uranium oxidation state, electronic absorption spectroscopy was employed. A weak, sharp f-f transition was observed at 1488 nm (ε = 136.6 M^{-1} cm^{-1}) indicative of U(V), Figure S10.
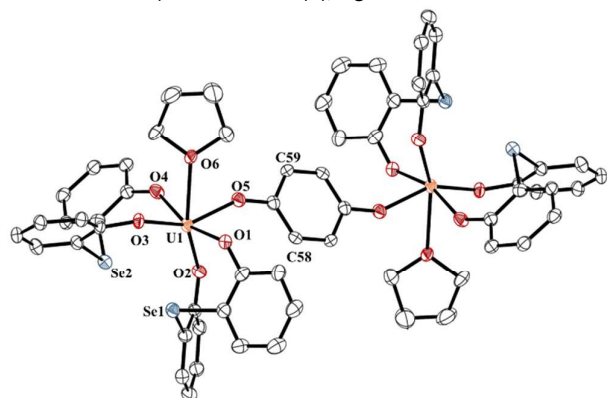
Figure 4. Thermal ellipsoid plot of **3** shown at the 50% probability level. The *tert*-butyl groups and hydrogen atoms have been omitted for clarity. The (μ_2-OC$_6$H$_4$O) moiety lies about an inversion centre.

The U-O$_{phenoxide}$ bond distances of **1,** 2.185(4)-2.223(4) Å, contract upon oxidation to **3**, 2.163(3)-2.140(3) Å. The U-O$_{phenoxide}$ distances in **3** are longer than the 2.02-2.03(1) Å found for the terminal U-O^{i}Pr distances in the U(V/V) dimer, U$_2$(O^{i}Pr)$_{10}$, and shorter than the 2.28-2.29(1) Å of the bridging U-O^{i}Pr bonds.[37] These distances are similar to those of U(V) aryloxide, [U(O^{t}Bu)$_6$]$^{1-}$, 2.05(1)-2.24(1) Å.[38]

The magnetic susceptibility of **3** is surprising. As illustrated in Figure S8, χT is linear from 10 K to 300 K, which indicates that only a single state is occupied or that multiple states are occupied, but their splitting is very small, < 2 K (1.2 cm^{-1}). Bonding in U(V) is expected to be more covalent than in U(IV) due to a better energy match between the metal and ligand orbitals; consequently, the ligand field in **3** expected to be strong relative to **1**. The ground

state of U(V) is ^{2}F$_{5/2}$, which consists of 6 substates with m$_j$ = -5/2, -3/2, ..., 5/2. The ligand field will mix with these substates based on the site symmetry of the U ion. In this case, the uranium centre has low symmetry, and the ^{2}F$_{5/2}$ state will split into 3 Kramers doublets. The magnetic moment of each Kramer's doublet is directly related to m$_J$ as shown in Table S2. The measured ground state moment of **3** is ~0.85 μ$_B$ per U center, which is not in agreement with any of the "pure" m$_J$ states. Given the low symmetry at the U centre and the fact that the relatively strong crystal field of U(V) will strongly mix the m$_J$ states, this result is not particularly surprising.

The most interesting aspect of the magnetic susceptibility of **3** is that only a single crystal field state is significantly occupied below 300 K, which is unusual for an actinide or lanthanide complex. In addition, the unpaired electrons on the two uranium centres are weakly exchange-coupled with 2J = -0.9 K/k$_B$ (-0.6 cm^{-1}).[39-41] This could be the reason why **3** was found to be EPR silent. The U1-O5-C57(quat) bond angle is 151.3(2)° deviates greatly from linearity, so this weak coupling is not surprising.

When the reaction of **2** with p-benzoquinone was attempted, no change was observed. The standard reduction potentials of p-benzoquinone, UO$_2$$^+$ and NpO$_2$$^+$ are 0.7 V, 0.45 V and 0.60 V, respectively.[42] Since Np(IV) is more difficult to oxidize than is U(IV), the potentials of p-benzoquinone and Np(V) are similar, and Np(V) aryloxide have been reported as being unstable,[12] this reaction between **2** and p-benzoquinone is not favourable.

The synthesis and spectroscopic characterization of U(IV) and Np(IV) aryloxides as well as their magnetism has been accomplished. This is the first Np(IV) EPR spectrum reported since 2004, and only the second Np(IV) aryloxide complex structure published to date. The reactivity of these complexes with p-benzoquinone has been studied. The U(IV) complex affords a rare dinuclear U(V)-U(V) compound, while the Np(IV) complex does not react. Overall, this represents a rare comparison of the reactivity of uranium and an element to the right of it in the periodic table.

Conflicts of interest
The authors declare no competing financial interests.

Notes and references

1   M. E. Fieser, C. T. Palumbo, H. S. La Pierre, D. P. Halter, V. K. Voora, J. W Ziller, F. Furche, K. Meyer, and W. J. Evans, *Chem. Sci.,* 2017, **8**, 7424-7433.
2   S. M. Mansell, N. Kaltsoyannis, and P. L. Arnold, *J. Am. Chem. Soc.,* 2011, **133**, 9036-9051.
3   I. Castro-Rodriguez, K. Olsen, P. Gantzel, and K. Meyer, *J. Am. Chem. Soc.,* 2003, **125**, 4565-4571.

4   C. J. Inman, A. S. P. Frey, A. F. R. Kilpatrick, F. G. N. Cloke, and S. M. Roe, *Organometallics*, 2017, **36**, 4539-4545.
5   J. Hümmer, F. W. Heinemann, and K. Meyer, *Inorg. Chem.*, 2017, **56**, 3201-3206.
6   B. Kosog, H. S. La Pierre, F. W. Heinemann, S. T. Liddle, and K. Meyer, *J. Am. Chem. Soc.,* 2012, **134**, 5284-5289.
7   W. G. Van der Sluys and A. P. Sattelberger, *Chem. Rev.*, 1990, **90**, 1027-1040.
8   S. D. McKee, C. J. Burns, and L. R. Avens, *Inorg. Chem.*, 1998, **37**, 4040-4045.
9   J. M. Berg, D. L. Clark, J. C. Huffman, D. E. Morris, A. P. Sattelberger, W. E. Streib, W. G. Van der Sluys, and J. G. Watkin, *J. Am. Chem. Soc.,*1992, **114**, 10811-10821.
10 E. Mora, L. Maria, B. Biswas, C. Camp, I. C. Santos, J. Pécaut, A. Cruz, J. M. Carrestas, J. Marçalo, and M. Mazzanti, *Organometallics*, 2013, **32**, 1409-1422.
11 M. W. Rosenzweig, F. W. Heinemann, L. Maron, and K. Meyer, *Inorg. Chem.*, 2017, **56**, 2792-2800.
12 E. T. Samulski, and D. G. Karraker, *J. Inorg. Nucl. Chem.,* 1967, **29**, 993-996.
13 A. C. Behrle, J. R. Levin, J. E. Kim, J. M. Drewett, C. L. Barnes, E. J. Schelter, and J. R. Walensky, *Dalton Trans.*, 2015, **44**, 2693-2702.
14 W. G. Van der Sluys, A. P. Sattelberger, W. E. Streib, and J. C. Huffman, *Polyhedron*, 1989, **8**, 1247-1249.
15 P. Pyykkö, *J. Phys. Chem. A*, 2015, **119**, 2326–2337.
16 A. T. Johnson, T. G. Parker, S. M. Dickens, J. K. Pfeiffer, A. G. Oliver, D. Wall, N. A. Wall, M. R. Finck, and K. P. Carney, *Inorg. Chem.*, 2017, **56**, 13553–13561.
17 D. J. A. De Ridder, C. Apostolidis, J. Rebizant, B. KanellaKopulos, and R. Maier, *Acta Crystallogr., Sect. C.: Cryst. Struct. Commun.,* 1996, **52**, 1436-1438.
18 Z. Zhang, B. F. Parker, T. D. Lohrey, S. J. Teat, J. Arnold, and L. Rao, *Dalton Trans.,* 2018, **47**, 8134-8141.
19 N. Magnani, C. Apostolidis, A. Morgenstern, E. Colineau, J.-C. Griveau, H. Bolvin, O. Walter, and R. Caciuffo, *Angew. Chem. Int. Ed.*, 2011, **50**, 1696-1698.
20 N. Magnani, E. Colineau, R. Eloirdi, J.-C. Griveau, R. Caciuffo, S. M. Cornet, I. May, C. A. Sharrad, D. Collison, and R. E. P. Winpenny, *Phys. Rev. Lett.,* 2010, **104**, 197202.
21 S. Stoll and A. Schweiger, *J. Magn. Reson.*, 2006, **178**, 42-55.
22 A. Jobiliong, Y. Oshima, J. S. Brooks and T. E. Albrecht-Schmitt, *Solid State Commun.*, 2004, **132**, 337-342.
23 I. Poirot, W. Kot, G. Shalimoff, N. Edelstein, M. M. Abraham, C. B. Finch and L. A. Boatner, *Phys. Rev. B*, 1988, **37**, 3255-3264.
24 G. Amoretti, D. C. Giori, G. Schianchi, G. Calestani, C. Rizzoli and J. C. Spirlet, *J. Less. Comm. Met.*, 1986, **122**, 35-45.
25 E. Gamp and N. Edelstein, *J. Chem. Phys.*, 1984, **80**, 5963-5967.
26 K. Rajnak, R. H. Banks, E. Gamp and N. Edelstein, *J. Chem. Phys.*, 1984, **80**, 5951-5962.
27 J. E. Butler and C. A. Hutchison Jr., *J. Chem. Phys.*, 1981, **74**, 3102-3119.
28 N. Edelstein, W. Kolbe and J. E. Bray, *Phys. Rev. B*, 1980, **21**, 338-342.
29 J. E. Bray, *Phys. Rev. B*, 1978, **18**, 2973-2977.
30 R. P. Richardson and J. B. Gruber, *J. Chem. Phys.*, 1972, **56**, 256-260.
31 A. F. Leung and E. Y. Wong, *Phys. Rev.*, 1969, **180**, 380-385.
32 F. Gendron, D. Páez-Hernández, F.-P. Notter, B. Pritchard, H. Bolvin and J. Autschbach, *Chem. Eur.J.*, 2014, **20**, 7994-8011.
33 D. Páez-Hernández and H. Bolvin, *J. Electron. Spec. Rel. Phenom.*, 2014, **194**, 74-80.
34 J. R. Robinson, C. H. Booth, P. J. Carroll, P. J. Walsh, and E. J. Schelter, *Chem. Eur. J.*, 2013, **19**, 5996-6004.
35 D. Werner, G. B. Deacon, P. C. Junk, and R. Anwander, *Chem. Eur. J.*, 2014, **20**, 4426-4438.
36 S. Hohloch, J. R. Pankhurst, E. E. Jaekel, B. F. Parker, D. J. Lussier, M. E. Garner, C. H. Booth, J. B. Love, and J. Arnold, *Dalton Trans.*, 2017, **46**, 11615-11625.
37 F. A. Cotton, D. O. Marler, and W. Schwotzer, *Inorg. Chem.*, 1984, **23**, 4211-4215.
38 S. Fortier, G. Wu, and T. W. Hayton, *Inorg. Chem.,* 2008, **47**, 4752-4761.
39 J. G. Brennan and R. A. Anderson, *J. Am. Chem. Soc.,* 1985, **107**, 514-516.
40 G. Nocton, P. Horeglad, J. Pécaut, and M. Mazzanti, *J. Am. Chem. Soc.*, 2008, **130**, 16633-16645.
41 L. P. Spencer, E. J. Schelter, P. Yang, R. L. Gdula, B. L. Scott, J. D. Thompson, J. L. Kiplinger, E. R. Batista, and J. M Boncella, *Angew. Chem. Int. Ed.,* 2009, **48**, 3795-3798.
42 L. R. Morss, N. M. Edelstein, and J. Fuger, *The Chemistry of the Actinide and Transactinide Elements*, Springer, Netherlands, 3rd edn, 2006, 2130.

131x56mm (150 x 150 DPI)